CMS Physics Analysis Summary

Contact: cms-pag-conveners-exotica@cern.ch 2012/08/19

Search for the associated production of unparticles and a Z boson in pp collisions at $\sqrt{s}$= 7 TeV in the final state containing muons and missing transverse energy

The CMS Collaboration

Abstract

This note describes a search for physics beyond the standard model in the final state $Z \to \mu\mu$ and missing transverse energy using a sample of proton-proton collision data at $\sqrt{s}$ = 7 TeV collected in 2011 with the CMS experiment, corresponding to an integrated luminosity of 4.98 fb^{-1} . The results are interpreted in an unparticle model. The data are found to agree with the standard model expectation, and upper limits on the unparticle model are set, significantly improving previous results.

The unparticle model was proposed by H. Georgi in 2007 [1]. Unparticles are a consequence of a scale invariant (conformal) sector with a non trivial infra-red fixed point that couples directly to the standard model fields at high energies. At an energy scale of Λ_U the interaction can be described by an effective Lagrangian [2] $\lambda \Lambda_U^{-d_U} O_{SM} O_U$, where O_{SM} is the standard model operator, O_U is the unparticle operator, and λ is a measure of the coupling between unparticles and the standard model fields. Although FCNC couplings are possible within the unparticle model, no FCNC couplings are considered in the used model. The parameters that define the unparticle physics are the scale Λ_U and the non-integer scale dimension d_U. From unitarity considerations one can set lower bounds on d_U [3], if conformal symmetry is conserved. A dimension above 2 would also be ultraviolet sensitive and is therefore not considered in the following. The unparticle model provides an environment to study particles with a continuous mass spectrum and unconventional signatures.

Limits on unparticle production have been derived, for example, for spin-1 unparticles, from measurements of electromagnetic dipole moments [4]. Previous direct searches for scalar unparticles produced in hadronic collisions have been performed using associated production with gluons and quarks (monojets) from CMS [5] and reinterpretations of extra dimension searches from CDF [6]. The CMS limits exclude scalar unparticles in a $\Lambda_U - d_U$ plane, up to $\Lambda_U = 18.9$ TeV for $d_U = 1.35$ and $\Lambda_U = 1$ TeV for $d_U = 1.7$ [5] . There were also reinterpretations of LEP measurements [7] in the Z/γ plus missing transverse energy ($E_{\mathrm{T}}^{\mathrm{miss}}$) channel. Using these data unparticles were excluded in ranges from $\Lambda_U = 69.5$ TeV for $d_U = 1$ to $\Lambda_U = 0.5$ TeV for $d_U = 2$ by assuming a Z boson coupling to the unparticle, and from $\Lambda_U = 25$ TeV for $d_U = 1$ to $\Lambda_U = 0.2$ TeV for $d_U = 2$ by assuming a coupling between the unparticles and the photon.

In the present analysis, we search for a scalar unparticle that couples to a standard model Z boson and leaves the detector without interaction (see Fig. 1). Only Z boson decays to $\mu^+\mu^-$ are considered. There are two types of standard model physics processes with this event signature, events with real $E_{\mathrm{T}}^{\mathrm{miss}}$ due to neutrinos that leave the detector, e.g. leptonic $\mathrm{t\bar{t}}$ or diboson decays, and processes with no neutrinos, but $E_{\mathrm{T}}^{\mathrm{miss}}$ as a result of detector effects, e.g. Drell-Yan (DY) production.

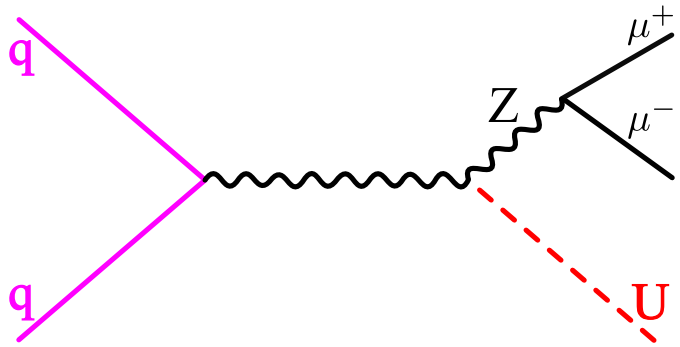

Figure 1: Feynman diagram of the studied model.

We use data from proton-proton collisions with a center-of-mass energy of 7 TeV recorded between March and October 2011, corresponding to an integrated luminosity of 4.98 fb^{-1}. Single muon triggers with isolation requirements were used to collect the events. The trigger thresholds varied between 17 GeV to 30 GeV over the course of the data taking period.

For the simulation of the background the MADGRAPH [8] generator was used for all processes except the $\mathrm{t\bar{t}}$ and single top processes, where POWHEG [9] was used. The standard model background at low $E_{\mathrm{T}}^{\mathrm{miss}}$ is dominated by the Drell-Yan process. At high $E_{\mathrm{T}}^{\mathrm{miss}}$ diboson events

and $t\bar{t}$ are dominant. The contributions from W+jet and multijet have been studied and were found to be negligible. The background predictions for diboson (ZZ,WZ,WW) and single top were normalised using next-to-leading order (NLO) QCD corrections [10]. For Drell-Yan next-to-next-to-leading order cross sections [11] were used, and next-to-next-to-leading order approximated cross sections for $t\bar{t}$ [12]. To produce the signal samples PYTHIA 8.145 [13] was used, which implements the unparticle model in leading order [14]. All simulated events have been passed through a full detector simulation based on GEANT4 [15]. The standard PYTHIA 8 parameters were used with the Tune 4C [16].

Events must have at least one good reconstructed vertex, with a distance to the beamspot of less than Δz =24 cm along the beam axis. To be above the trigger threshold, one muon must have $p_T > 32$ GeV reconstructed from a global fit to the hits in the central tracker and the muon system. Both muons have to be reconstructed in the good fiducial region of the muon system $|\eta| < 2.1$. The pseudorapidity is defined by $\eta = -\ln(\tan(\theta/2))$. The second muon has a p_T threshold of 17 GeV. The track associated with each muon has to satisfy certain quality cuts. It must have at least one hit in the pixel detector, more than ten hits in the tracker and at least two hits in the muon chambers. The χ^2/N_{dof} has to be smaller than 12. To select isolated muons, the relative track isolation $(\sum_{\Delta R<0.3} p_T)/p_T^{\mu}$ has to be less than 10%, where $(\sum_{\Delta R<0.3} p_T)$ is the sum over all charged particles within a $\Delta R = 0.3$ cone ($\Delta R = \sqrt{(\Delta\eta)^2 + (\Delta\phi)^2}$) around the muon track, excluding the muon itself. To reject cosmic muons, the minimal distance of the track in the x-y plane (d_0) to the primary vertex has to be smaller than 0.2 cm. The cosine of the solid angle between the two muons has to be bigger than 0.02 . Finally, a distance $\Delta R > 0.5$ between a muon and the nearest jet is required to reduce muons from heavy flavor decays.

Electrons are used to veto events with additional leptons. Well identified electrons are selected in the ECAL barrel ($|\eta| < 1.44$) or in the ECAL endcaps ($1.566 < |\eta| < 2.5$) of the detector and must have $E_T > 20$ GeV.

Jets are clustered from objects, reconstructed with the particle flow algorithm [17][18], using the anti-k_T algorithm with a distance parameter of 0.5. Only jets above a p_T threshold of 30 GeV and with $|\eta| < 3$ are considered. The corrections on the jet energy scale [19] are applied. If these jets have less than 2 constituents and more than 99% contribution from neutral hadrons, they are rejected as well as jets that are consistent with being an electron or photon. The E_T^{miss} is defined as the negative vectorial sum over all objects reconstructed by the particle flow algorithm. CMS has several levels of correction available for particle flow E_T^{miss} [20]. In this preliminary analysis, the corrections for the jet energy scale were not applied, since part of the jet energy scale corrections are obtained from events containing either a photon or a Z [19], and there is the possibility that the presence of signal might bias their determination. Because the energy scale is known to differ between data and simulation [19], this results in a small discrepancy between the data and simulation. An ad hoc correction, based on the total $\sum E_T$ in the event and described below, was applied to account for this.

To reduce non-Z backgrounds, a Z boson candidate is selected by requiring two muons that pass all the selection criteria and have opposite electric charge. The invariant mass must be within 20 GeV of the nominal Z boson mass (see Fig. 2). The Z candidate and E_T^{miss} have to be back to back in the transverse plane: $\Delta\phi(p_T^Z, E_T^{miss}) \geq 2$. Events with additional muons or electrons are rejected, using the same identification criteria as above. To reduce the systematic uncertainties due to mismeasured jets, and enhance the signal, we only select events with less than two jets (see Fig. 2). The contribution from $t\bar{t}$ is further reduced by rejecting events containing any b tagged jet with $p_T > 50$ GeV. For b tagging, the track counting high efficiency algorithm [21] was used, with a mistag rate of 2.86%. The final discriminant between signal

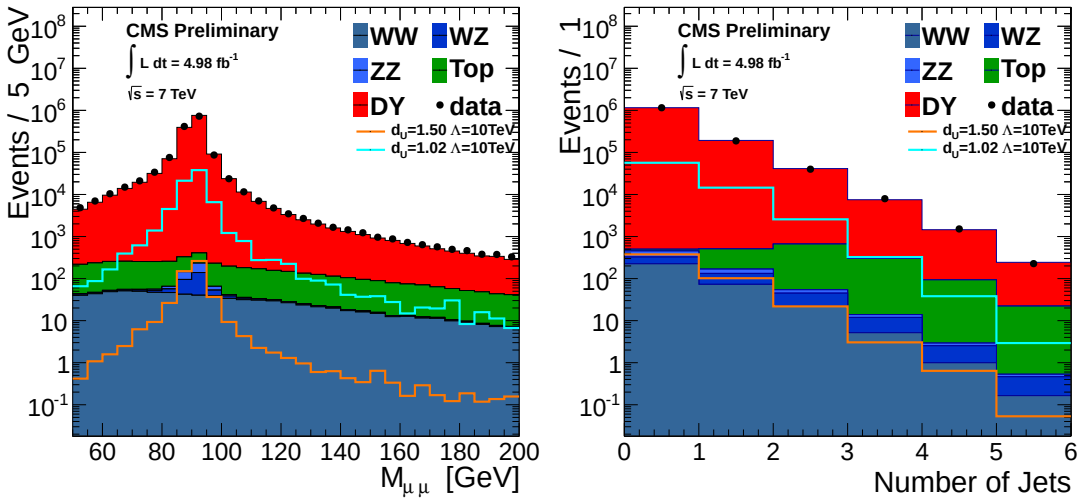

Figure 2: In the left distribution the invariant mass of two selected muons is shown. The N_{jet} distribution for events with a invariant mass of 20 GeV around the Z mass is shown on the right. Background processes are shown as stacked histograms. Two typical signal models are overlaid on the plots.

and background is $E_{\mathrm{T}}^{\mathrm{miss}}$. The $E_{\mathrm{T}}^{\mathrm{miss}}$ was required to be greater than 100 GeV, as this gives the best expected exclusion limit. A summary of the predicted backgrounds from the simulation at different stages in the selection, as well as the number of events in the data, are given in Table 1. Some of the backgrounds are further evaluated using data-driven methods as described in the following and the data-driven backgrounds, when available, are used in the calculation of the limit.

An important irreducible background to this analysis is ZZ $\rightarrow 2l2\nu$ production, which has the same signature in the detector as the expected signal. Of similar magnitude is the Drell-Yan background, where the $E_{\mathrm{T}}^{\mathrm{miss}}$ is due to the detector response. Several systematic uncertainties on the $E_{\mathrm{T}}^{\mathrm{miss}}$ in Drell-Yan events have been considered and will be discussed below. Processes with two bosons containing at least one W boson are suppressed by the kinematic requirements listed before. Events from WZ processes only have large $E_{\mathrm{T}}^{\mathrm{miss}}$ if the W boson decays leptonically and are reduced by vetoing events with an additional muon or electron that satisfies the quality criteria. All processes with two W-bosons such as $\mathrm{t\bar{t}}$, WW and single top (tW-channel) are strongly suppressed by the selection criteria.

The contribution from $\mathrm{t\bar{t}}$ and WW production is derived from a control sample of $e\mu$ events ($e\mu$-method). Because of lepton universality, processes with two decaying W bosons have the same kinematics for $\mu\mu$ and $e\mu$ final states. The $E_{\mathrm{T}}^{\mathrm{miss}}$ distribution is therefore expected to have the same shape in both channels and twice the number of events in the $e\mu$-channel after correcting for the different electron and muon reconstruction and identification efficiencies, using a correction factor denoted $R_{\mu\mu} = N_{\mu\mu}/N_{e\mu}$.
The factor $R_{\mu\mu}$ is taken from a sideband in the invariant mass distributions with little Drell-Yan event contribution ($M_Z + 20\,\mathrm{GeV} < M_{\mu\mu} < M_Z + 60\,\mathrm{GeV}$). In order to further increase the $\mathrm{t\bar{t}}$ purity, one jet is required to be b tagged. The value of $R_{\mu\mu}$ is determined to be $R_{\mu\mu} = 0.47 \pm 0.04$ (stat) ± 0.03 (syst). To extract the top and WW events in the signal region, we apply the signal event selection to all $e\mu$ events, and rescale the obtained distribution with the factor $R_{\mu\mu}$. There are 78 events in the $e\mu$-channel after the event selection, see Fig. 3 (left). In the signal region 0.5 ± 0.05 (stat) events from WZ processes are subtracted based on the WZ prediction

Table 1: Standard model prediction from simulation for different requirements. Uncertainties are statistical. The numbers of events observed in the data are also given.

	2 OS μ	$\lvert M_{\mu\mu} - M_Z \rvert < 20\,\text{GeV}$	$N_{jet} < 2$	$\Delta\phi(Z, E_\text{T}^\text{miss}) \geq 2$	No b-Jet	$E_\text{T}^\text{miss} > 100\,\text{GeV}$
WW	889 ± 4.7	326 ± 2.8	298 ± 2.7	237 ± 2.4	237 ± 2.4	6.60 ± 0.4
WZ	223 ± 0.9	192 ± 0.8	160 ± 0.7	116 ± 0.6	116 ± 0.6	12.2 ± 0.2
ZZ	280 ± 0.8	260 ± 0.8	250 ± 0.8	214 ± 0.8	214 ± 0.8	29 ± 0.3
Top	$4.90\text{k} \pm 17.5$	$1.76\text{k} \pm 11$	716 ± 10	491 ± 8.7	421 ± 8.6	28.2 ± 0.9
DY	$1.46\text{M} \pm 0.9\text{k}$	$1.40\text{M} \pm 0.9\text{k}$	$1.35\text{M} \pm 0.9\text{k}$	$597\text{k} \pm 580$	$595\text{k} \pm 580$	9.0 ± 2.3
Total bgrd.	$1.47\text{M} \pm 0.9\text{k}$	$1.4\text{M} \pm 0.9\text{k}$	$1.35\text{M} \pm 0.9\text{k}$	$598\text{k} \pm 580$	$596\text{k} \pm 580$	78.6 ± 2.5
Data	1.47M	1.39M	1.34M	620k	618k	88
$d_U = 1.9$ $\Lambda = 10\,\text{TeV}$	53 ± 0.2	51 ± 0.2	47 ± 0.2	44 ± 0.2	44 ± 0.2	16 ± 0.2

from simulation. Finally, 37 ± 5.6 (stat + syst) events are predicted. This result is compatible with the simulation, where 28 ± 1 (stat) ± 3 (syst) events are expected. In Fig. 3 (right) the final

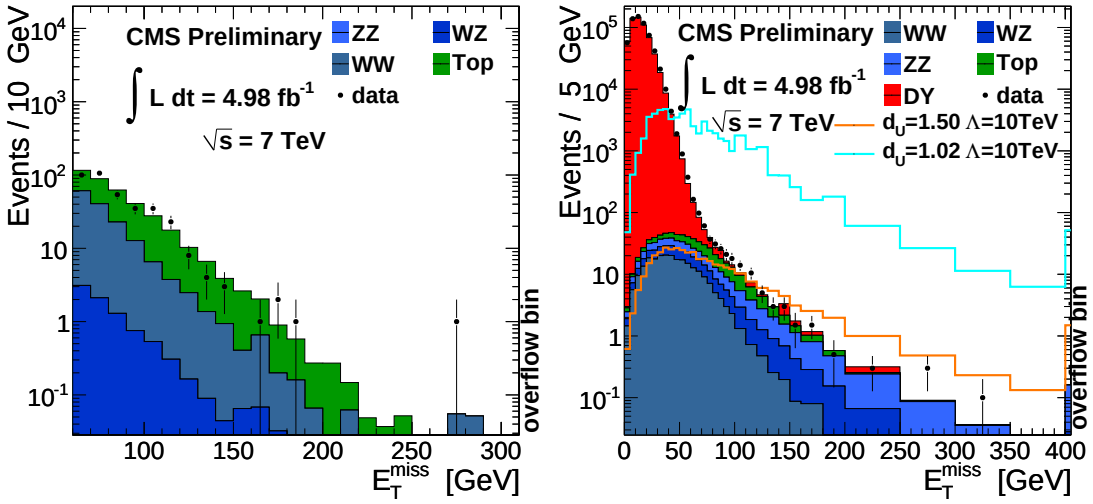

Figure 3: The distribution of E_T^miss in the $e\mu$-channel with the signal selection applied (left) and $\mu\mu$-channel with all cuts except E_T^miss (right). In the right plot, in addition to the simulated SM background and the data, we show two exemplary signal distributions.

E_T^miss distribution before requiring $E_\text{T}^\text{miss} > 100\,\text{GeV}$ is shown. The data are found to be well described by the background expectation.

The systematic uncertainties on the final event yield are calculated using the uncertainties for each object and estimating the influence on E_T^miss. The object uncertainties are: muon momentum scale and muon p_T resolution have uncertainties of 0.1% and 0.5%, respectively [22]. The electron energy scale is known to 1.3% in the barrel and 4.1% in the endcaps [23]. The η and p_T dependent jet energy scale and the uncertainty on the jet energy resolution (10%) are also taken into account [19]. The effect of these uncertainties on the number of expected events in the signal region is shown in Table 2.

To quantify the effect of the unclustered energy, defined as energy in the detector not reconstructed as objects, the E_T^miss resolution in Drell-Yan events is studied. The E_T^miss resolution is evaluated as a function of $\sum E_\text{T}$, defined as the scalar sum of the transverse energy from all

Table 2: Impact of object related uncertainties on the expected number of events in the search region.

	Jet energy resolution	Jet energy scale	Muon	Electron
Background	5.6%	5.2%	$< 0.1\%$	$< 0.1\%$
Signal	5%	0.8%	$< 0.1\%$	$< 0.1\%$

particle flow objects. The resolution function agrees in data and simulation. A difference is observed in the $\sum E_{\mathrm{T}}$ distribution, where a shift between simulation and data of $2.52 \pm 0.01\,\mathrm{GeV}$ (stat) per reconstructed vertex is found. The impact of this shift on the $E_{\mathrm{T}}^{\mathrm{miss}}$ resolution is interpreted as systematic uncertainty. The influence on the background expectation used from the simulation is 5%, while the signal shows no significant effect. In the present analysis $E_{\mathrm{T}}^{\mathrm{miss}}$ is reconstructed without the application of jet energy corrections (JEC), because the JEC might have a small bias due to the signal. The absence of JEC is accounted for by a systematic uncertainty on $E_{\mathrm{T}}^{\mathrm{miss}}$, which translates into an 8% uncertainty on backgrounds estimated from Monte Carlo simulation and a 1% uncertainty on signal.

In addition to the systematic influence from the unclustered energy, there is an uncertainty on the number of pile up interactions observed in data and generated in simulation. To estimate this, the number of simulated pile up interactions is varied by $\pm 5\%$, resulting in a 5% variation in the background prediction and a 4% variation in the signal.

The parton distribution functions (PDF) used in the event simulation have a systematic influence on the predicted background. To estimate this effect the PDF uncertainties for CTEQ6.6 [24], MSTW08 [25] and NNPDF2.1 [26] were used to reweight the distributions using the LHAPDF package [27]. This procedure follows the recommendations of the PDF4LHC working group [28]. The envelope of the considered PDF error sets with respect to the central value of each set was used as uncertainty on the background. Additional uncertainties due to α_s were calculated using the same method, yielding a total PDF uncertainty of 3.4% on the number of predicted background events from Monte Carlo in the search region and a 3% uncertainty for the signal yield.

The luminosity uncertainty is 2.2% [29]. The b-tagging uncertainty has been found to have an influence of $< 1\%$, and therefore can be neglected. The muon reconstruction and identification efficiency uncertainties are 2% [30]. The trigger efficiency is found to agree within 1% in data and Monte Carlo simulation. For the background contributions determined from the Monte Carlo simulation, an additional uncertainty of 4% was included as theoretical uncertainty on the cross section predictions, leading to an uncertainty of 2% on the total background prediction.

A summary of the systematic uncertainties from the different sources on the search region is shown in Table 3.

The total event prediction from simulation for the standard model background is 79 ± 9. For top and WW events we use the data-driven background estimation of 37 ± 5.6 events. Further backgrounds are estimated by the simulation to be 52 ± 7.5. This leads to a total standard model prediction of 88 ± 9.4 events. In the data 88 events are observed. The signal efficiency does only depend weakly on Λ_U, and is about $9 \pm 1\%$ in the d_U range 1 up to 1.3 and rises to 16% for $d_U = 1.9$.

Table 3: Summary of all systematic uncertainties on the number of events in the signal region.

	Background MC	Signal
Jet resolution and scale	5%	2%
Unclustered energy	5%	3%
$E_{\mathrm{T}}^{\mathrm{miss}}$ corrections	8%	1%
Pile up	3%	1%
PDF	3%	3%
Cross sections	2%	-
Efficiencies	3%	
Luminosity	2%	

The number of observed events agrees with the background expectation, therefore we set limits on the signal cross section. Different parameter points were tested by varying the unparticle model parameter d_U with a fixed Λ_U and λ, which have no influence on the signal efficiency. 95% C.L. exclusion limits are set on the model. The $\mathrm{CL_s}$ method [31] was used with a profile likelihood test statistic where the number of expected events μ is:

$$\mu = B + \varepsilon\sigma\mathcal{L}.$$

Here, B is the number of expected background events, ε is the signal efficiency, σ is the signal cross section and $\mathcal{L}$ is the luminosity. The probability of the number of observed events is modelled by a Poisson likelihood:

$$L(n|\mu,\theta) = \frac{\mu^n e^{-\mu}}{n!} \cdot \pi(\theta),$$

where $\pi(\theta)$ is the function to constrain the nuisance parameters, and is chosen to be a log-normal-function. The results are interpreted in the d_U and Λ_U plane with the coupling constant λ set to one. The interpretation for the $d_U \to 1$ limit is not straightforward for a fixed $\lambda = 1$, because the cross section becomes independent of Λ_U. Therefore we also interpret the result for a fixed Λ_U and a non constant value of λ. By comparing the excluded cross section with the predicted LO cross sections of the unparticle model, limits are set on the model parameters d_U and Λ_U as shown in Fig. 4 and the results in the d_U and λ plane is shown in Fig. 5.

The excluded values of Λ_U as a function of the scale dimension d_U are listed in Table 4 and can be seen in Fig. 4. The coupling constant λ is set to unity for this interpretation. These limits extend the previous limits in this channel from LEP [7] that exclude unparticles with $\Lambda_U = 5$ TeV at $d_U = 1.35$ to $\Lambda_U = 0.6$ TeV at $d_U = 1.9$. The searches in the monojet channel at CMS [5] exclude unparticles with $\Lambda_U = 18.9$ TeV at $d_U = 1.35$ and $\Lambda_U = 1$ TeV at $d_U = 1.7$.
The results for the interpretation of a fixed Λ_U in the d_U and λ plane are summarized in Table 5 and Figure 5.

In conclusion, we presented a search for signatures of a scale invariant sector in the Z+$E_{\mathrm{T}}^{\mathrm{miss}}$ final state, in a sample of proton proton collisions collected with the CMS experiment at $\sqrt{s} = 7$ TeV. The data were taken in 2011 and correspond to an integrated luminosity of 4.98 fb^{-1}. $E_{\mathrm{T}}^{\mathrm{miss}}$ was used to discriminate between the standard model Drell-Yan process and the associated production of a Z-boson with an unparticle. The background expectation from $\mathrm{t\bar{t}}$ and WW events to the signal region was determined from the data using $e\mu$ events, and was found to be

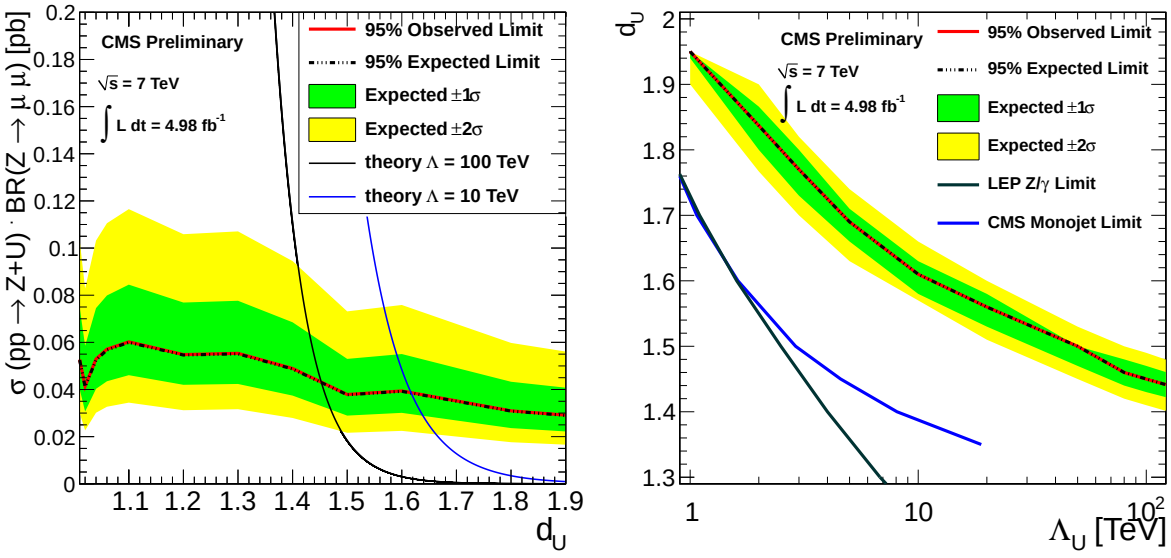

Figure 4: The expected and observed CL_s limits improve slightly with increasing d_U (left). The CL_s limit translated into the model parameter plane of Λ_U and d_U (right). For the parameter values below the curve the 95% CL cross section limit is less than the theoretical cross section.

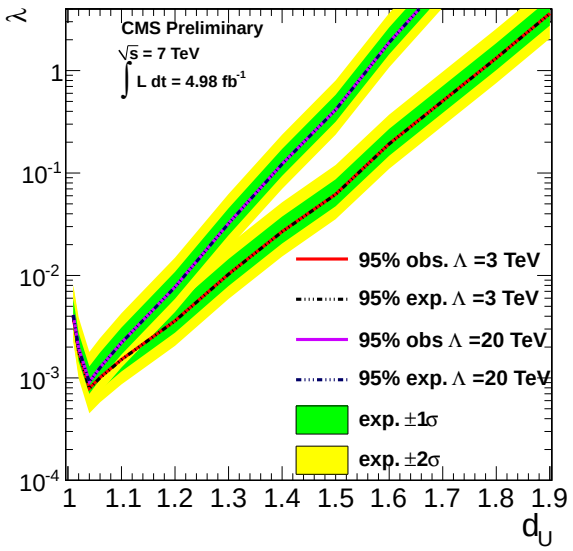

Figure 5: The CL_s limit translated into the plane of λ and d_U . For the parameter values above the curve the 95% CL cross section limit is less than the theoretical cross section.

consistent with the prediction from the simulation.
The observed number of events with $E_T^{miss} > 100\,GeV$ was found to be in agreement with the standard model prediction. Limits have been set on the unparticle model, for values of the scaling dimension d_U between 1 and 1.9 at 95% CL. The disfavored values of λ are in the range of $8 \cdot 10^{-4}$ for $d_U = 1.04$ up to 0.19 for $d_U = 1.6$ at $\Lambda_U = 3\,TeV$. For a fixed coupling constant $\lambda = 1$ values of d_U can be excluded from $d_U = 1.45$ with $\Lambda_U = 100\,TeV$ up to $d_U = 1.95$ with $\Lambda_U = 1\,TeV$. This is a significant improvement in comparison to previous direct searches and the first search in this channel at the LHC.

Table 4: Expected and observed 95% CL limits on d_U as a function of Λ_U.

Λ_U[TeV]	obs. d_U	exp. d_U
1	1.95	1.95
2	1.84	1.84
3	1.77	1.77
5	1.69	1.69
10	1.61	1.61
20	1.56	1.56
50	1.50	1.50
80	1.46	1.46
100	1.45	1.45

Table 5: Expected and observed 95% CL limits on λ as a function of d_U.

d_U	$\Lambda_U = 3$ TeV		$\Lambda_U = 20$ TeV	
	obs. λ	exp. λ	obs. λ	exp. λ
1.04	$7.9{\cdot}10^{-4}$	$7.9{\cdot}10^{-4}$	$9.2{\cdot}10^{-4}$	$9.1{\cdot}10^{-4}$
1.06	$1.0{\cdot}10^{-3}$	$1.0{\cdot}10^{-3}$	$1.3{\cdot}10^{-3}$	$1.3{\cdot}10^{-3}$
1.09	$1.2{\cdot}10^{-3}$	$1.2{\cdot}10^{-3}$	$1.8{\cdot}10^{-3}$	$1.7{\cdot}10^{-3}$
1.10	$1.5{\cdot}10^{-3}$	$1.5{\cdot}10^{-3}$	$2.2{\cdot}10^{-3}$	$2.2{\cdot}10^{-3}$
1.20	$3.6{\cdot}10^{-3}$	$3.6{\cdot}10^{-3}$	$7.7{\cdot}10^{-3}$	$7.7{\cdot}10^{-3}$
1.30	0.010	0.010	0.032	0.032
1.40	0.027	0.027	0.12	0.12
1.50	0.062	0.062	0.41	0.41
1.60	0.19	0.19	1.9	1.9

References

[1] H. Georgi, "Unparticle Physics", *Physical Review Letters* **98** (2007), no. d, 9, doi:10.1103/PhysRevLett.98.221601, arXiv:0703260.

[2] K. Cheung, W.-Y. Keung, and T.-C. Yuan, "Collider Phenomenology of Unparticle Physics", *Physical Review D* **76** (2007), no. 5, 37, doi:10.1103/PhysRevD.76.055003, arXiv:0706.3155.

[3] B. Grinstein, K. Intriligator, and I. Z. Rothstein, "Comments on Unparticles", *Physics Letters* **B662** (2008), no. 4, 367–374, doi:10.1016/j.physletb.2008.03.020, arXiv:0801.1140.

[4] A. Moyotl, A. Rosado, and G. Tavares-Velasco, "Lepton electric and magnetic dipole moments via lepton flavor violating spin-1 unparticle interactions", *Physical Review D* **84** (2011), no. 7, 14, doi:10.1103/PhysRevD.84.073010, arXiv:1109.4890.

[5] CMS Collaboration Collaboration, "Search for New Physics with a Mono-Jet and Missing Transverse Energy in pp Collisions at sqrt(s) = 7 TeV", *Phys.Rev.Lett.* **107** (2011) 201804, doi:10.1103/PhysRevLett.107.201804, arXiv:1106.4775.

[6] A. Delgado and M. J. Strassler, "A Simple-Minded Unitarity Constraint and an Application to Unparticles", *Phys. Rev.* **D81** (2010) 056003, doi:10.1103/PhysRevD.81.056003, arXiv:0912.2348.

[7] S. Kathrein, S. Knapen, and M. J. Strassler, "Bounds from LEP on unparticle interactions with electroweak bosons", *Phys.Rev.* **D84** (2011) 015010, doi:10.1103/PhysRevD.84.015010, arXiv:1012.3737.

[8] J. Alwall, P. Demin, S. de Visscher et al., "MadGraph/MadEvent v4: The New Web Generation", *JHEP* **0709** (2007) 028, doi:10.1088/1126-6708/2007/09/028, arXiv:0706.2334.

[9] C. Oleari, "The POWHEG-BOX", *Nucl.Phys.Proc.Suppl.* **205-206** (2010) 36–41, doi:10.1016/j.nuclphysbps.2010.08.016, arXiv:1007.3893.

[10] J. M. Campbell and R. Ellis, "An Update on vector boson pair production at hadron colliders", *Phys.Rev.* **D60** (1999) 113006, doi:10.1103/PhysRevD.60.113006, arXiv:hep-ph/9905386.

[11] R. Gavin, Y. Li, F. Petriello et al., "FEWZ 2.0: A code for hadronic Z production at next-to-next-to-leading order", *Comput.Phys.Commun.* **182** (2011) 2388–2403, doi:10.1016/j.cpc.2011.06.008, arXiv:1011.3540.

[12] N. Kidonakis, "Higher-order corrections to top-antitop pair and single top quark production", arXiv:0909.0037.

[13] T. Sjostrand, S. Mrenna, and P. Z. Skands, "A Brief Introduction to PYTHIA 8.1", *Comput.Phys.Commun.* **178** (2008) 852–867, doi:10.1016/j.cpc.2008.01.036, arXiv:0710.3820.

[14] S. Ask, "Simulation of Z plus Graviton/Unparticle Production at the LHC", *The European Physical Journal C* **60** (2008), no. 3, 11.

[15] J. Allison, K. Amako, J. Apostolakis et al., "Geant4 developments and applications", *IEEE Trans.Nucl.Sci.* **53** (2006) 270, doi:10.1109/TNS.2006.869826.

[16] R. Corke and T. Sjostrand, "Interleaved Parton Showers and Tuning Prospects", *JHEP* **03** (2011) 032, doi:10.1007/JHEP03(2011)032, arXiv:1011.1759.

[17] CMS Collaboration, "Particle-Flow Event Reconstruction in CMS and Performance for Jets, Taus, and Missing ET", *CMS Physics Analysis Summary CMS PAS PFT-09-001* (2009).

[18] CMS Collaboration, "Commissioning of the Particle-Flow Reconstruction in Minimum-Bias and Jet Events from pp Collisions at 7 TeV", *CMS Physics Analysis Summary CMS PAS PFT-09-002* (2010).

[19] CMS Collaboration, "Determination of Jet Energy Calibration and Transverse Momentum Resolution in CMS", *JINST* **6** (2011) P11002, doi:10.1088/1748-0221/6/11/P11002, arXiv:1107.4277.

[20] CMS Collaboration, "Missing transverse energy performance of the CMS detector", *J. Instrum.* **6** (2011) P09001. 56 p, arXiv:1106.5048.

[21] CMS Collaboration, "Performance of the b-jet identification in CMS", *CMS Physics Analysis Summary CMS PAS-BTV-11-001* (2011).

[22] CMS Collaboration, "Performance of the CMS muon detector with pp collisions $\sqrt{s}$ = 7 TeV/c^2 at the LHC", *CMS Physiscs Analysis Summery CMS-PAS-MUO-10-002* (2010).

[23] CMS Collaboration, "A search for excited leptons in pp Collisions at sqrt(s) = 7 TeV", *Phys. Lett.* **B704** (2011) 143–162, doi:10.1016/j.physletb.2011.09.021, arXiv:1107.1773.

[24] P. M. Nadolsky, H.-L. Lai, Q.-H. Cao et al., "Implications of CTEQ global analysis for collider observables", *Phys.Rev.* **D78** (2008) 013004, doi:10.1103/PhysRevD.78.013004, arXiv:0802.0007.

[25] A. Martin, W. Stirling, R. Thorne et al., "Parton distributions for the LHC", *Eur.Phys.J.* **C63** (2009) 189–285, doi:10.1140/epjc/s10052-009-1072-5, arXiv:0901.0002.

[26] NNPDF Collaboration Collaboration, "Unbiased global determination of parton distributions and their uncertainties at NNLO and at LO", *Nucl.Phys.* **B855** (2012) 153–221, doi:10.1016/j.nuclphysb.2011.09.024, arXiv:1107.2652.

[27] M. R. Whalley, D. Bourilkov, and R. C. Group, "The Les Houches Accord PDFs (LHAPDF) and Lhaglue", arXiv:hep-ph/0508110.

[28] M. Botje, J. Butterworth, A. Cooper-Sarkar et al., "The PDF4LHC Working Group Interim Recommendations", arXiv:1101.0538.

[29] CMS Collaboration, "Absolute Calibration of Luminosity Measurement at CMS: Summer 2011 Update", *CMS Physiscs Analysis Summery CMS-PAS-EWK-11-001* (2011).

[30] CMS Collaboration, "Search for New Physics in Highly Boosted Z0 Decays to Dimuons in pp Collisions at sqrt(s)=7 TeV", *CMS Physiscs Analysis Summery CMS-PAS-EXO-10-025* (2011).

[31] A. L. Read, "Presentation of search results: the CLs technique", *Journal of Physics G: Nuclear and Particle Physics* **28** (2002), no. 10, 2693.